

New SPB stars in the field of the young open cluster NGC 2244 discovered by the MOST^{*} photometric satellite.

D. Gruber^{1,2†}, H. Saio^{3‡}, R. Kuschnig¹, L. Fossati⁴, G. Handler⁵, K. Zwintz¹,
W. W. Weiss¹, J. M. Matthews⁶, D. B. Guenther⁷, A. F. J. Moffat⁸, S.M. Rucinski⁹,
D. Sasselov¹⁰

¹University of Vienna, Institute for Astronomy, Türkenschanzstrasse 17, A-1180 Vienna, Austria

²Max Planck Institut für Extraterrestrische Physik, Giessenbachstrasse, D-85748 Munich, Germany

³Astronomical Institute, Graduate School of Science, Tohoku University, Sendai, 980-8578, Japan

⁴Department of Physics and Astronomy, Open University, Walton Hall, Milton Keynes MK7 6AA, UK

⁵Nicolaus Copernicus Astronomical Center, Bartycka 18, 00-716 Warsaw, Poland

⁶Department of Physics and Astronomy, University of British Columbia, 6224 Agricultural Road, Vancouver, BC V6T 1Z1, Canada

⁷Department of Astronomy and Physics, St. Mary's University, Halifax, NS B3H 3C3, Canada

⁸Département de physique, Université de Montréal C.P. 6128, Succursale Centre-Ville, Montréal, QC H3C 3J7, Canada

⁹Department of Astronomy & Astrophysics, David Dunlap Observatory, University of Toronto P.O. Box 360, Richmond Hill, ON L4C 4Y6, Canada

¹⁰Harvard-Smithsonian Center for Astrophysics, 60 Garden Street, Cambridge, MA 02138, USA

ABSTRACT

During two weeks of nearly continuous optical photometry of the young open cluster NGC 2244 obtained by the MOST satellite, we discovered two new SPB stars, GSC 00154-00785 and GSC 00154-01871. We present frequency analyses of the MOST light curves of these stars, which reveal two oscillation frequencies (0.61 and 0.71 c/d) in GSC 00154-00785 and two (0.40 and 0.51 c/d) in GSC 00154-01871. These frequency ranges are consistent with g-modes of $\ell \leq 2$ excited in models of main-sequence or pre-main-sequence (PMS) stars of masses 4.5 - 5 M_{\odot} and solar composition (X, Z) = (0.7, 0.02). Published proper motion measurements and radial velocities are insufficient to establish unambiguously cluster membership for these two stars. However, the PMS models which fit best their eigenspectra have ages consistent with NGC 2244. If cluster membership can be confirmed, these would be the first known PMS SPB stars, and would open a new window on testing asteroseismically the interior structures of PMS stars.

Key words: stars: early-type – stars: pre-main sequence – stars: individual:GSC 00154-00785 and GSC 00154-01871 – stars: oscillations – open clusters and associations: individual: NGC 2244

1 INTRODUCTION

Slowly pulsating B (SPB) stars pulsate in high-order, low-degree gravity modes with periods of the order of a few days, showing dense frequency spectra, low amplitudes and multi-periodicity with beat periods of months and even years (Waelkens et al. 1987; Waelkens 1991). The effective temperature range of known SPB stars is 10,000 - 20,000 K; the mass range is 3 - 8 solar masses. SPB

pulsations are driven by the κ -mechanism of the Fe opacity bump at $T \approx 1.5 \times 10^5$ K (Gautschy & Saio 1993; Dziembowski et al. 1993). Being trapped deep inside the star, SPB g-modes are very promising for asteroseismology of massive stars (De Cat 2007). Currently, there are at least 50 confirmed SPB stars and 65 candidate SPB stars in our Galaxy, 60 in the LMC and 11 in the SMC (Kołaczowski et al. 2006).

Since SPB stars have periods of a few days, it can be difficult to characterise their eigenspectra accurately with data from ground-based observatories due to aliasing caused by daily gaps in the time series. Space-based photometry, with long, nearly uninterrupted time coverage, is essential to perform the best frequency analyses for asteroseismology.

The MOST (Microvariability & Oscillations of STars) mission, Canada's first space telescope, obtains highly precise optical photometry of bright stars ($V < 10^m$) nearly continuously over

* Based on data from MOST, a Canadian Space Agency mission operated by Microsat Systems Canada Inc. (formerly the space division of Dynacon, Inc.) and the University of Toronto Institute for Aerospace Studies and the University of British Columbia, with the assistance of the University of Vienna.

† E-mail: dgruber@mpe.mpg.de (DG)

‡ E-mail: saio@astr.tohoku.ac.jp (HS)

time spans up to 60 days (Walker et al. 2003). Within two years of MOST's launch in 2003, the satellite's capabilities were expanded to include photometry of the Guide Stars for each Primary Science Target field. Many variable stars have been discovered in this large, nearly random, Guide Star sample ($9 < V < 6$), spread across the HR Diagram.

In January 2008, MOST observed the very young open cluster NGC 2244. Embedded in the Rosette Nebula, NGC 2244 is located in the vicinity of the Galactic anti-center ($l = 206.306$ $b = -2.072$) at a distance estimated to be in the range of $1.4 \leq D[\text{kpc}] \leq 1.7$ (see Ogura & Ishida 1981; Perez et al. 1987; Hensberge et al. 2000; Park & Sung 2002; Bonatto & Bica 2009).

The age of the cluster was first estimated to be 2 – 4 Myr (see Chen et al. 2007, and references therein); a more recent estimate allows a broader range of 0.2 - 6 Myr (Bonatto & Bica 2009). While many of the cluster stars appear to be younger than 3 Myr, about 45% of the cluster members may be older than 3 Myr, indicating an earlier epoch of star formation (Bergöfer & Christian 2002). Of the younger portion of the sample, 5% are estimated to be significantly younger than 3 Myr, suggesting star formation is ongoing in NGC 2244.

GSC 00154-00785 and GSC 00154-01871 were used as Guide Stars for the NGC 2244 field and were found to be variable. The data analyses presented in this paper show the stars to be SPB stars similar to HD 163830, the first SPB star discovered by MOST (Aerts et al. 2006) In Sect.2, we give a short description of the photometry, and in Sect.3, our analysis techniques and results. Sect.4 deals with evidence for the cluster membership of both stars. Section 5 describes the theoretical models which best fit the observed pulsations, and we present discussion and our conclusions in Sect.6.

2 OBSERVATION AND DATA REDUCTION

The MOST satellite monitored GSC 00154-00785 (B9V, $V=10.93$, $\alpha = 6^h 33^m 35.7^s$, $\delta = 5^\circ 16' 41''$) and GSC 00154-01871 (B5V, $V=11.30$, $\alpha = 6^h 33^m 43.3^s$, $\delta = 4^\circ 55' 54''$) as guide stars for science observations of the NGC 2244 cluster field. Fig. 1 and 2 show the light curves of GSC 00154-00785 and GSC 00154-01871, respectively. Both light curves clearly show several simultaneous oscillations with periods near 2 days.

For the NGC 2244 observations 30 subsequent exposures were co-added ('stacked') onboard the satellite with a respective exposure time of 2.03 s. This results in a total sampling period, i.e. the time between consecutive photometric measurements, of 60.9 s. GSC 00154-00785 was guide star #35 and GSC 00154-01871 was guide star # 36 during this observation run.

Stray light due to scattered Earthshine reaches the focal plane of the MOST Science CCD, and this background is modulated with the orbital frequency of the satellite (14.2 c/d) and some of its harmonics. (See Reegen et al. 2006 for a discussion of this effect.) The Guide Star photometric data were folded in phase at the period of the MOST orbit (about 101 min) to treat the orbital modulation of the stray light background. Data points most strongly affected by stray light and other outliers were rejected from the light curve. To account for the changing nature of the Earth's albedo beneath the moving satellite, this process was performed with consecutive segments of the light curve, each four MOST orbits long.

We draw attention to a decrease in relative flux of about 0.02 mag apparent in all the stars in the NGC 2244 field during JD-JD2000 = 2936 - 2940 (and noticeable in Figures 1 and 2). Al-

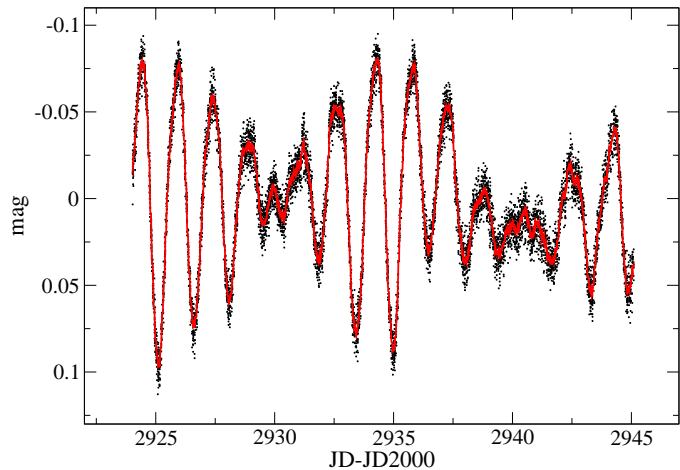


Figure 1. Light curve of GSC 00154-00785 obtained by MOST photometry for 21 days after subtracting the mean magnitude. The red solid line shows a boxcar running average with a smoothing length of 50 s.

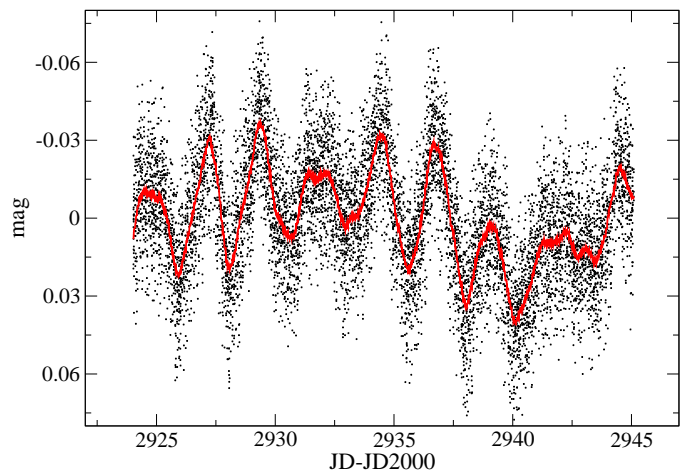


Figure 2. Same as Fig. 1 but for GSC 00154-01871. The red solid line shows a boxcar running average with a smoothing length of 200 s.

though this artefact does not affect our pulsational frequency analyses below, we do conservatively neglect any frequencies in the time series with $f \leq 0.25$ c/d, since we cannot be sure they are intrinsic to a given star.

3 DATA ANALYSIS

3.1 Time series analysis

For our frequency search, we employed *Period04*¹ (Lenz et al. 2005). *Period04* is a code specifically designed to extract multiple periodic signals in astronomical time series through simultaneous least squares fitting.

The assessment of the signal-to-noise ratio (S/N) for a given amplitude in general is a complex task. With *Period04*, a mean amplitude is determined in an interval centered on the frequency of interest which is then compared to the amplitude of the peak in question. Obviously, the result depends on the chosen interval

¹ <http://www.univie.ac.at/tops/Period04/>

GSC 00154-00785			
	f [c/d]	σ	amp [mmag]
f_1	0.608	± 0.048	38.2
f_2	0.705	± 0.048	32.0
f_3	$(f_1 + f_2)$	± 0.048	6.9
GSC 00154-01871			
	f [c/d]	σ	amp [mmag]
f_1	0.407	± 0.048	17.6
f_2	0.514	± 0.048	8.20

Table 1. Frequencies and combination frequencies of GSC 00154-00785 and GSC 00154-01871 with errors estimated according to $\sigma = T^{-1}$, and amplitudes (amp).

which may contain non-noise signal due to intrinsic frequencies, side-lobes, etc. Vaughan (2005) introduced a method (used by e.g. Gruber et al. 2011) with which one can estimate whether quasi-periodic-pulsations (QPPs) are indeed significant. We applied this method to check which amplitudes exceed the 3.8σ limit commonly used in asteroseismology and find 3 and 2 frequencies passing this requirement for GSC 00154-00785 and GSC 00154-01871, respectively.

To determine the uncertainties, we use the well known Rayleigh criterion ($\sigma_f = T^{-1}$, with T being the data set length), which is a conservative estimate of the frequency error as was demonstrated by Kallinger et al. (2008).

Table 1 lists the oscillation frequencies and uncertainties, as well as the associated amplitudes that we obtained using the methodology outlined above. Figures 3 and 4 show the corresponding amplitude and power density spectra. The number of identified frequencies is small compared to other known SPB stars, as e.g. HD 163830 (Aerts et al. 2006), HD 163868 (Walker et al. 2005), and HD 163899 (Saio et al. 2006). This deficit may be due to a larger noise level of our observations in the frequency domain due to a data set, which is approximately half as long as that for the 3 mentioned SPB stars. Additionally, the resulting lower frequency resolution reduces the capability of identifying closely spaced frequencies.

De Cat (2007, and references therein) argues that amplitude spectra of SPB stars with only a few dominant modes can be explained partially or even entirely by stellar rotation, a concept which was elaborated more recently by Balona et al. (2011) for γ Dor stars. If future observations of GSC 00154-00785 and GSC 00154-01871 do not unravel additional low-amplitude frequencies, they would indeed be candidates for such an explanation. However, if one considers the observed $v \sin i$ of about 8 km/s (see Section 3.2), one finds that GSC 00154-00785 and GSC 00154-01871 would need to have an inclination angle, i , of about 4 to 5 degree in order to explain the observed frequencies due to rotation. Assuming a random distribution of i the probability of finding a star with $i < 5$ is $P = 1 - \cos(5)$ which translates to $P \approx 0.4\%$. At this point we cannot rule out this explanation for our observed frequency spectra. But we stress that it is rather unlikely that rotational modulation is the cause for the observed periodicities. In any case, SPB stars with few pulsation frequencies, or few frequencies dominating significantly the frequency spectrum pose a challenge to theory and provide an interesting observational fact in itself.

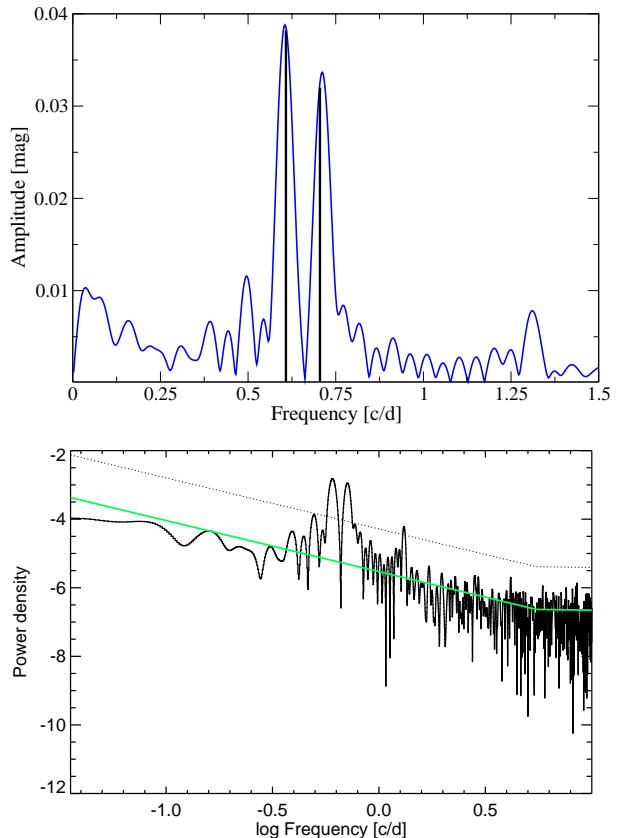


Figure 3. Upper panel: Region of interest of the amplitude spectrum of GSC 00154-00785 (blue) with the identified frequencies (black). Lower panel: Amplitude spectrum in log – log space. Shown are the broken power-law fit to the data (green solid line) and the 3.8σ limit (dashed line)

3.2 Atmospheric parameters.

For both stars Strömgen $uvby\beta$ photometry is available (Handler 2011). Applying the calibrations by Napiwotzki et al. (1993) to the data provide the atmospheric parameters which are listed in Table 2. GSC 00154-01871 is a spectroscopic binary (see Huang & Gies 2006), therefore the $H\beta$ measurement is highly affected by its companion and thus, not useful to determine $\log g$.

We also analysed high-resolution ($R \cong 48000$) spectra of the two stars obtained during 6 - 8 December 2008 with the FEROS spectrograph, installed on the 2.2 m ESO telescope at La Silla, Chile (Kaufer et al. 2000). FEROS is a cross-dispersed, fibre-fed echelle spectrograph. Typical signal-to-noise ratios of the spectra (covering wavelengths from 3800 to 9100 Å) range from 100 to 150. From the FEROS spectra of these stars, provided to us by Niemczura (priv. comm.), we obtain similar parameters to those listed in Table 2, and we confirm that GSC 00154-01871 is indeed a spectroscopic binary. From the spectral analysis we also report a $v \sin i$ of about 8 km/s for both stars. The corresponding results of the spectroscopic observations will be the subject of a forthcoming paper (Niemczura et al., in preparation).

The average atmospheric parameters (from Strömgen photometry and from spectroscopy), presented in boldface in Table 2, will be used in the remainder of this paper.

Table 2. Atmospheric parameters for both GSC 00154-00785 and GSC 00154-01871 determined from Strömgen photometry and spectroscopy.

Star	T_{eff} [K]	$\log g$ [cm/s ²]	ref.
GSC 00154-00785	14400 ± 300	4.0 ± 0.2	Niemczura (priv. comm.)
	14800 ± 600	4.3 ± 0.2	Handler (2011)
	14600 ± 330	4.15 ± 0.15	average
GSC 00154-01871	13800 ± 300	3.8 ± t.b.d	Niemczura (priv. comm.)
	13605 ± 59	3.80 ± 0.01	Huang & Gies (2006)
	14300 ± 600	4.4 ± 0.2	Handler (2011)
	13900 ± 360	3.8 ± 0.15	average ^a

^a for the average of $\log g$ the value obtained from photometry was excluded because H β is strongly affected by the companion.

Table 3. Proper motion and radial velocity of the NGC 2244 open cluster and the two target stars: GSC 00154-00785 and GSC 00154-01871. All values, besides the stellar radial velocity, are taken from Kharchenko et al. (2004) and Kharchenko et al. (2005). The radial velocity of GSC 00154-01871 is missing because the star is a spectroscopic binary and we do not have enough spectra to measure a reliable mean radial velocity.

	RA [J2000]	DEC [J2000]	$\mu_{\alpha} \cos(\delta)$ [mas/yr]	$\sigma_{\mu_{\alpha} \cos(\delta)}$ [mas/yr]	μ_{δ} [mas/yr]	$\sigma_{\mu_{\delta}}$ [mas/yr]	V_{rad} [km/s]	$\sigma_{V_{\text{rad}}}$ [km/s]
NGC 2244	06 31 55	+04 56 30	-1.42	0.39	-0.32	0.37	26.16	3.37
GSC 00154-00785	06 33 36	+05 16 41	+1.87	1.90	-4.26	2.60	28.2	1
GSC 00154-01871	06 33 43	+04 55 54	-1.16	1.78	-3.21	1.70	--	--

4 FIELD STARS OR CLUSTER MEMBERS?

4.1 Proper motion study and radial velocity

To establish membership through a proper motion study, NGC 2244 is not an easy cluster to investigate, due to both its rather large distance and the similarity between the proper motions of stars in the cluster and those in the field, as is illustrated in the atlas of NGC 2244 published by Kharchenko et al. (2005). According to this atlas, the cluster member proper motions are concentrated around a mean of $(-1.42, -0.32)$ mas/yr, compared to the mean for field stars in the same region of the sky of $(+0.92, -6.55)$ mas/yr with a dispersion for the cluster stars of $\sigma_{\mu_{AC}} = 4.45 \pm 0.15$ mas/yr (Kharchenko et al. 2004; Chen et al. 2007).

Table 3 shows a comparison between the cluster mean values of proper motion and radial velocity for NGC 2244 and those of the two target stars: GSC 00154-00785 and GSC 00154-01871. From their independent proper motion study, Chen et al. (2007) estimate membership probability for GSC 00154-00785 to be 50%, and for GSC 00154-01871, 84%.

For GSC 00154-00785, the measurements of both $\mu_{\alpha} \cos(\delta)$ and μ_{δ} agree with those of the cluster within 2σ . The agreement of $\mu_{\alpha} \cos(\delta)$ values improves if one considers only the 30 cluster members listed by Kharchenko et al. (2004) with measurement uncertainties smaller or comparable to those of GSC 00154-00785. In that sub-sample, the dispersion of $\mu_{\alpha} \cos(\delta)$ is approximately 2.5 mas/yr. The agreement between the cluster mean values and those of the two stars is as satisfactory for GSC 00154-00785 as it is for the most precisely measured stars in the cluster.

The agreement between the mean cluster radial velocity (Kharchenko et al. 2005) and the value given for GSC 00154-01871 by Niemczura (priv. comm.) strengthens the case for mem-

bership of this star. However, we do not include this star's radial velocity in Table 3, because the star is a spectroscopic binary (Huang & Gies 2006) and we do not have enough spectra over time to be able to provide a very accurate mean radial velocity of the binary system. For GSC 00154-01871, we arrive at the same conclusion as for GSC 00154-00785, but even more strongly, since the star's value of $\mu_{\alpha} \cos(\delta)$ agrees with the cluster mean to within only 1σ .

4.2 Reddening and CMD analysis

In Fig. 6 we show the positions of the two stars relative to the central region of NGC 2244.

Applying the calibration by Crawford (1978) to the Strömgen colour indices gives $E(b - y) = 0.245$ and $M_v = -0.09 \pm 0.4$ for GSC 00154-00785 and $E(b - y) = 0.379$, $M_v = 0.15 \pm 0.4$ for GSC 00154-01871. The considerably lower reddening of GSC 00154-00785 is understandable given its position in the outer parts of the region of NGC 2244. With V magnitudes of 10.93 and 11.30 respectively (Handler 2011), we obtain distances of 980 ± 400 and 800 ± 350 pc for GSC 00154-00785 and GSC 00154-01871, respectively.

The distance of NGC 2244 is estimated to fall in the range of 1.4 - 1.7 kpc (see Bonatto & Bica 2009, and references therein). Our Strömgen results put the two stars at roughly half the cluster distance and thus argue against cluster membership. However, we point out that the distances we derive for the stars are within 1σ of the lowest estimate of the cluster distance.

Words of warning: If either star is surrounded by circumstellar matter, this would redden the stars, making the Crawford (1978) calibration routine invalid. However, neither of the two stars

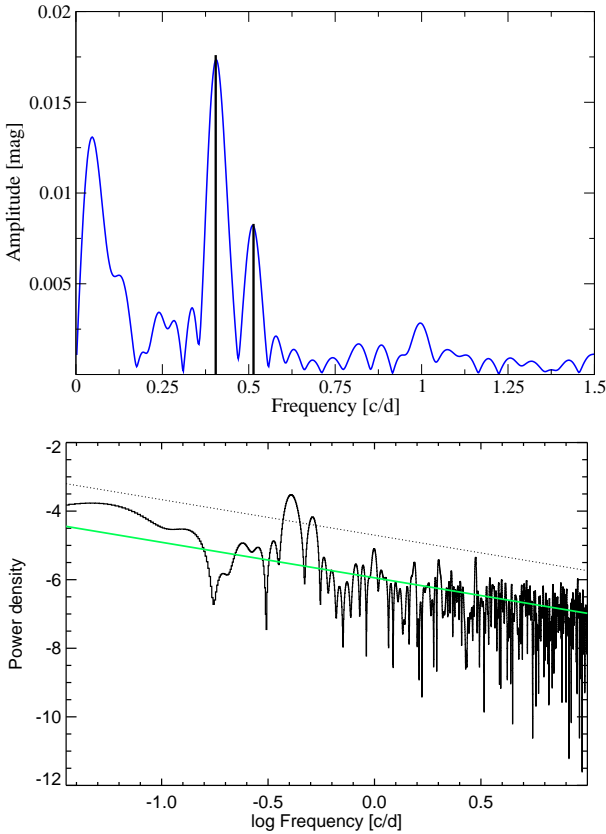


Figure 4. *Upper panel:* Region of interest of the amplitude spectrum of GSC 00154-00785 (blue) with the identified frequencies (black). *Lower panel:* Amplitude spectrum in log – log space. Shown are the power-law fit to the data (green solid line) and the 3.8σ limit (dashed line)

shows emission lines in its spectrum (Niemczura priv. comm.). GSC 00154-01871 is a spectroscopic binary and therefore its absolute magnitude derived from *uvby* photometry cannot be trusted. For B stars, the latter is calibrated via $H\beta$ whose value is affected by the presence of a companion.

The calibration routine implicitly assumes that the two stars are main-sequence (MS) stars. If these stars are in their pre-main sequence (PMS) stage, we argue that the Crawford (1978) routine can be safely applied because (a) there is no evidence for circumstellar emission, and (b) the colour excesses from the *uvby* photometry are not anomalous.

Figure 5 is a dereddened colour-magnitude diagram (CMD) containing stars from the samples of Heiser (1977); Perez et al. (1989); Kaltcheva et al. (1999); Hensberge et al. (2000) and Handler (2011). These have a membership probability $> 85\%$ (cross-checked against Marshall et al. 1982; Kharchenko et al. 2005; Baumgardt et al. 2000 and Chen et al. 2007). The dereddened colour index $(b - y)_0$ and V_0 were obtained using the Crawford (1978) calibration as described above. The unsuspecting position of GSC 00154-00785 and GSC 00154-01871 in the CMD as well as their location in the field of NGC 2244 supports cluster membership of the two stars.

4.3 Conclusion of this section

Neither the cluster membership determinations nor the distance estimates are iron-clad, and they suffer from qualifiers and caveats.

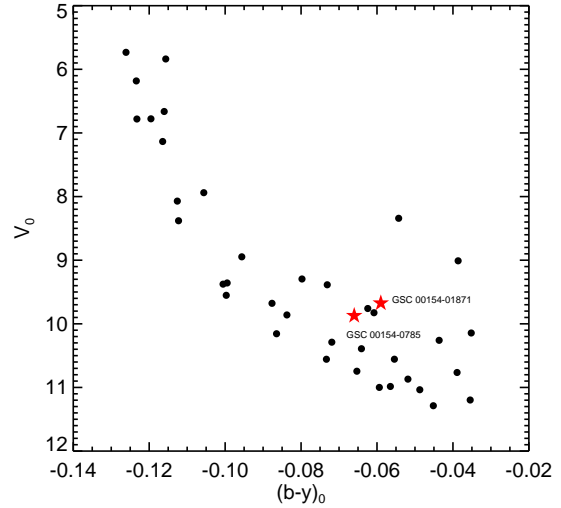


Figure 5. Zoom into the dereddened colour-magnitude diagram (CMD) for cluster members of NGC 2244. Positions of GSC 00154-00785 and GSC 00154-01871 are superimposed (red stars).

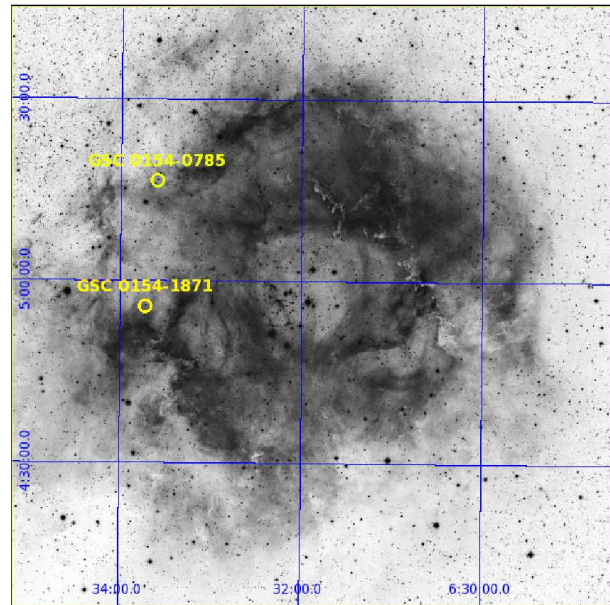


Figure 6. POSS-I image of NGC 2244 observed at a wavelength of $\sim 0.5 \mu\text{m}$. Green circles denote the positions of the two guide stars, GSC 00154-00785 and GSC 00154-01871.

Although, membership of GSC 00154-00785 and GSC 00154-01871 is possible, we are unable to confirm it. GAIA parallaxes will settle this issue.

5 MODELS

5.1 Evolutionary models

GSC 00154-00785

The effective temperature and surface gravity derived in Sect. 3.2 are plotted in the bottom panel of Fig. 7 with main-sequence (MS)

evolutionary tracks² (solid lines) and pre-main-sequence (PMS) tracks (dashed lines). This diagram indicates that GSC 00154-00785 has a mass of $4.5 \pm 0.5 M_{\odot}$ no matter whether it is an MS or PMS star.

We can estimate the age of the star by comparing its position on the $\log g - \log T_{\text{eff}}$ diagram with the evolutionary tracks. If the star is assumed to be a MS star, its age is 20 – 50 Myr.

Assuming it to be a *field star*, thus using the absolute magnitude derived from Strömgen photometry (Sect. 4.2), and applying a bolometric correction of -1.14 (Flower 1996), we find $M_{\text{bol}} = -1.23 \pm 0.4$ which corresponds to a luminosity of $\log L/L_{\odot} = 2.42 \pm 0.16$. However, if GSC 00154-00785 is a *cluster member*, adopting a distance modulus of $(m - M)_0 = 11.1$ for NGC 2244 (see e.g. Park & Sung 2002, and references therein) we find $M_{\text{bol}} = -2.27$, corresponding to a luminosity of $\log L/L_{\odot} = 2.8 \pm 0.25$.

GSC 00154-01871

The position of GSC 00154-01871 in Fig. 7 is also based on the parameters derived in Sect. 3.2. The location of this star in Fig. 7 suggests that this star has a mass of $5.0 \pm 0.5 M_{\odot}$, whether it is an MS or PMS star. If the star is assumed to be an MS star, its age is 70 – 80 Myr.

We estimate the luminosity as above for GSC 00154-00785. With a bolometric correction of -1.02 (Flower 1996), we find for GSC 00154-01871 the following values: $M_{\text{bol}} = -0.87$ and a luminosity of $\log L/L_{\odot} = 2.28 \pm 0.16$. On the other hand, GSC 00154-01871 has a stronger case for *cluster membership*. If we adopt the same distance modulus as for GSC 00154-00785 above and after applying a bolometric correction of -1.02 (Flower 1996) we find a bolometric magnitude of $M_{\text{bol}} = -2.45$ and a corresponding luminosity of $\log L/L_{\odot} = 2.91 \pm 0.25$.

If we assume that GSC 00154-01871 is a field star, the evolutionary models that best fit this star in a $\log L - \log T_{\text{eff}}$ plot conflict with what is expected from the $\log g - \log T_{\text{eff}}$ diagram shown in Fig. 7. On the other hand, the stellar masses derived from the evolutionary models are consistent in both diagrams if the star is assumed to be a cluster member. Additionally, if the star is in the field, its luminosity would be only marginally consistent with models of g-mode excitation. Both points are circumstantial evidence to support the membership of GSC 00154-01871 in NGC 2244.

Implications: MS or PMS?

If these stars are on the MS, the estimated ages are much larger than the age range for the open cluster NGC 2244 (0.2 – 6 Myr Bonatto & Bica 2009). This argues against a cluster membership if they are MS stars. However, if the stars are still in their PMS stage, the situation is different. The dashed lines in Fig. 7 show PMS evolutionary tracks. The initial model for each PMS track has been obtained by accreting mass starting from a $1 M_{\odot}$ model on the Hayashi track. As seen in Fig. 7, both stars can be identified as PMS stars with masses near $4.5 M_{\odot}$. The ages are estimated for GSC 00154-01871 and GSC 00154-00785 to be about 0.2 Myr and 0.4 Myr, respectively, after termination of mass accretion. If the stars are indeed cluster members, then their location in the HRD implies that they must be PMS stars. In the following, pulsational analyses, we consider the g-mode pulsation spectra in both MS and

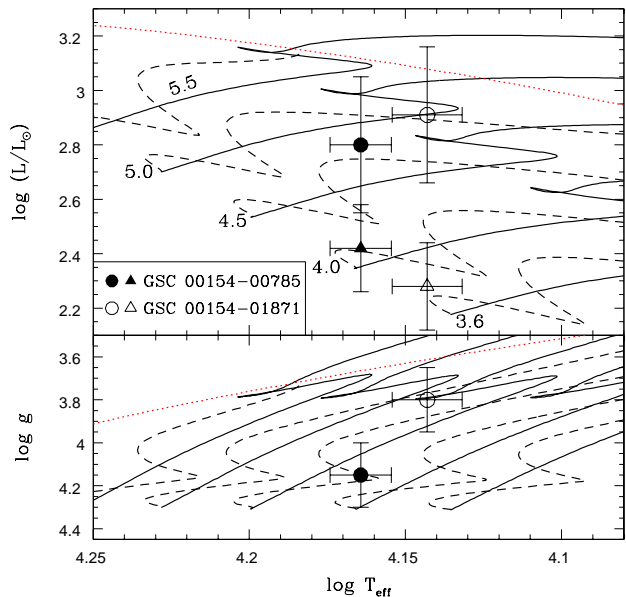


Figure 7. Estimated parameters for GSC 00154-00785 (filled symbols) and GSC 00154-01871 (open symbols) are compared with evolutionary models in the HR diagram (top panel) and in the $\log g - \log T_{\text{eff}}$ diagram. The two positions for each star in the top panel correspond to the two kinds of estimates for the luminosity discussed in the text: circles denote the luminosity assuming the stars to be cluster members, triangles denote the field star assumption. Dashed lines are PMS evolution tracks, while solid lines are MS and post-MS evolution tracks for each stellar mass indicated (in solar units) along each track in the top panel. Dotted lines indicate the approximate locus of the birth line.

PMS models. (A detailed discussion about g-modes in PMS stars can be found in Appendix A.)

5.2 Pulsation models

Fig. 8 shows oscillation frequencies of excited low-degree $\ell = 1$ and $\ell = 2$ modes along the evolutionary tracks of non-rotating $4.5 M_{\odot}$ models in MS (left panel) and in PMS (right panel) stages. We have adopted a standard chemical composition ($X = 0.7$, $Z = 0.02$) with OP opacity tables (Badnell et al. 2005). In a casual inspection of Fig. 8, no significant differences in the range of excited g-mode frequencies are evident between MS and PMS models. Both types of models with similar effective temperatures excite g-modes with similar periods, because the excitation occurs in outer layers of the star. Before a convective core appears in the PMS stage (around the peak in luminosity), the amplitudes of g-modes in the deep interior are much larger than in MS models, although the number of nodes (a few tens) are not large enough to significantly dissipate g-mode oscillations as in the post-main-sequence models. The g-mode spectra for PMS models are simpler than those for MS models because of the absence of mode crossings associated with the gradient in mean molecular weight found after the ZAMS.

The range of excited frequencies shifts downward as the effective temperature decreases, and for a given effective temperature the frequency range is slightly smaller for PMS models. Those trends are due mainly to the difference in stellar radii of the mod-

² Evolutionary models were computed by a standard Henyey type code.

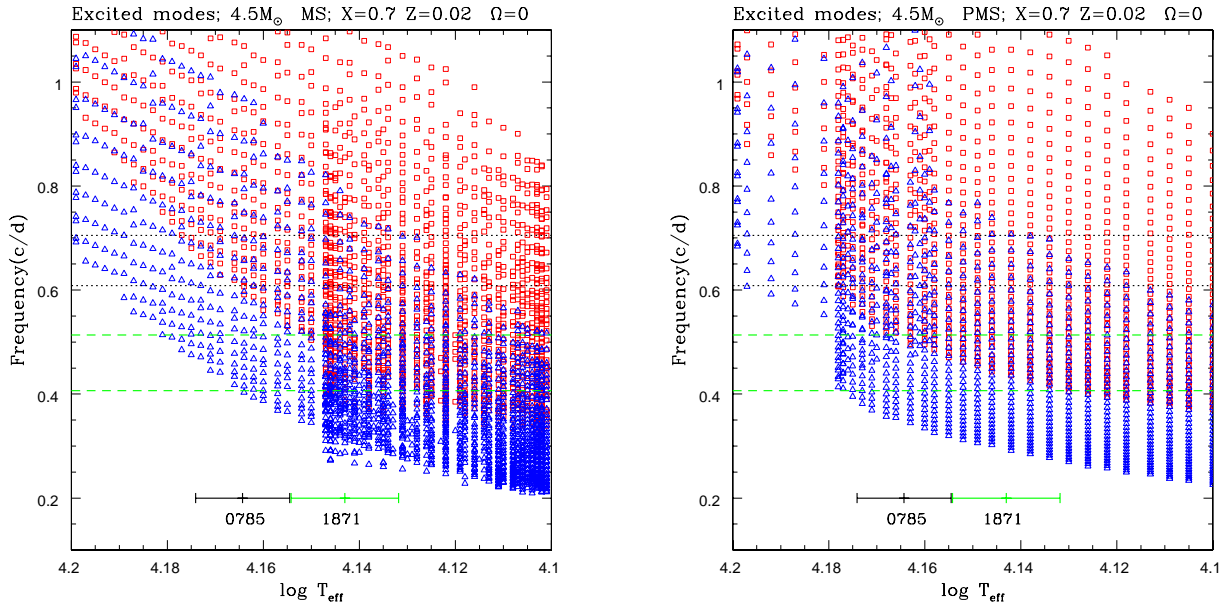


Figure 8. Frequencies of excited high-order, low-degree $\ell = 1$ (blue triangles) and $\ell = 2$ (red squares) g-modes versus effective temperature for the $4.5 M_{\odot}$ evolution models in the MS (left panel) and in the PMS (right panel) phases. Horizontal dotted and dashed lines indicate frequencies detected in GSC 00154-00785 and GSC 00154-01871, respectively. The cross and the horizontal line in the lower part of each diagram indicates the estimated effective temperatures with error bars for GSC 00154-00785 and GSC 00154-01871.

els; the frequency of a g-mode is lower for a star of larger radius. Fig. 8 shows that, for both MS and PMS models, the frequency range of excited $\ell = 1$ and 2 modes covers well the ranges of oscillation frequencies detected in GSC 00154-01871 (dashed lines) and GSC 00154-00785 (dotted lines).

If GSC 00154-00785 and/or GSC 00154-01871 are PMS stars, evolutionary period (frequency) change is expected to be more rapid than in the MS stage. Fig. 9 shows the rates of period change dP/dt for selected g-modes in the $4.5 M_{\odot}$ model during PMS evolution.

At the effective temperature of GSC 00154-00785 ($\log T_{\text{eff}} = 4.164$), the periods are expected to increase with time, while at the effective temperature of GSC 00154-01871 ($\log T_{\text{eff}} = 4.143$), they decrease. The period decrease is caused by the PMS contraction, while the increase is caused by the fact that Brunt-Väisälä frequency decreases deep in the star with the development of a convective core which first appears at $\log T_{\text{eff}} \approx 4.15$.

If GSC 00154-00785 and GSC 00154-01871 are PMS stars, Fig. 9 indicates that the period change rates is ~ 1 sec/yr and ~ -0.2 sec/yr, respectively. Such period changes might be detectable by an (O-C) diagram based on long baseline observations.

6 CONCLUSIONS

MOST has revealed the SPB nature of stars (GSC 00154-00785 and GSC 00154-01871) in the same part of the sky as the very young open cluster NGC 2244. The main pulsation periods of these multi-periodic SPB stars are near 2 days. The ranges of pulsation frequencies of the stars is consistent with nonradial g-modes low degree ($\ell = 1$ and $\ell = 2$) excited by the kappa mechanism at the Fe bump.

The effective temperatures and surface gravities we derive

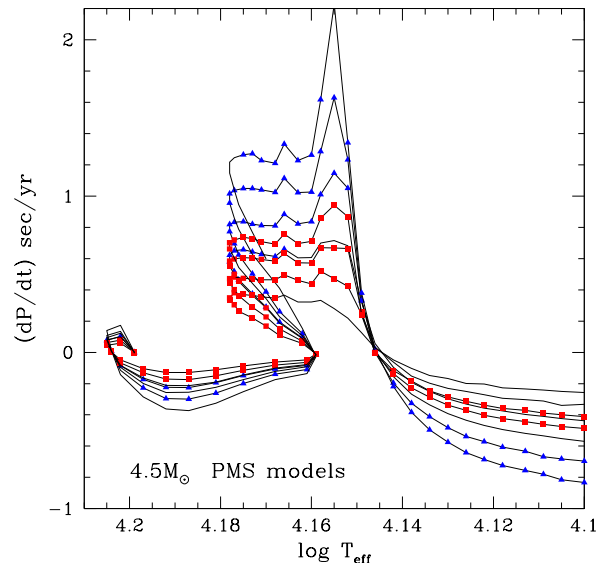


Figure 9. The rates of period change for some g-modes in the $4.5 M_{\odot}$ model during the PMS evolution. Plotted modes are g_{15} , g_{20} , g_{25} and g_{30} for $\ell = 1$ and 2. (Longer period modes tend to have larger $|dP/dt|$.) Filled triangles and squares indicate modes for $\ell = 1$ and 2, respectively to be excited.

from Strömgren indices and spectroscopy indicate the two stars have masses of about $4.5 - 5.0 M_{\odot}$. If GSC 00154-00785 and GSC 00154-01871 are MS stars, our estimates for their ages are 20 – 50 Myr and 70 – 80 Myr, respectively, much older than the cluster NGC 2244 (0.2 – 6 Myr). If the two stars are still in the PMS

stage, they would be a few tenths of Myr after the end of the protostellar accretion phase. Therefore, if these stars are proven members of NGC 2244, then almost certainly they are PMS stars. Existing proper motion and radial velocity properties of the two pulsators cannot establish reliably their membership in the NGC 2244 cluster. GAIA parallaxes and proper motions should eventually remove this uncertainty.

If the membership to NGC 2244 can be indeed confirmed, GSC 00154-00785 and GSC 00154-01871 would be the first known PMS SPB pulsators. This possibility has alerted us to begin a more concerted search with MOST and other space photometry missions for other SPB pulsators among PMS cluster and field stars.

ACKNOWLEDGMENTS

The authors are grateful to Ewa Niemczura for useful discussion and the analysis of the Feros spectra. We dedicate this work to the memory of our dear friend and colleague Dr. Piet Reegen, who will be greatly missed by us all. Astronomy research at the Open University is supported by an STFC rolling grant (L.F.). GH is partially supported by the Austrian Fonds zur Förderung der wissenschaftlichen Forschung under grant P20526-N16 and WW by P22691-N16. KZ is recipient of an APART fellowship of the Austrian Academy of Sciences at the Institute of Astronomy of the University Vienna. J.M.M., A.F.J.M., and S.M.R. are funded by NSERC (Canada) and some of R.K.'s contributions were partially funded by the Canadian Space Agency.

REFERENCES

- Aerts, C., De Cat, P., Kuschnig, R., Matthews, J. M., Guenther, D. B., Moffat, A. F. J., Rucinski, S. M., Sasselov, D., Walker, G. A. H., & Weiss, W. W., 2006, *ApJ*, 642, L165
- Badnell N. R., Bautista M. A., Butler K., Delahaye F., Mendoza C., Palmeri P., Zeppen C. J., & Seaton M. J., 2005, *MNRAS*, 360, 458
- Balona, L. A., Guzik, J. A., Uytterhoeven, K., Smith, J. C., Tenenbaum, P., & Twicken, J. D., 2011, *MNRAS*, 415, 3531
- Baumgardt H., Dettbarn C., & Wielen R., 2000, *A&AS*, 146, 251
- Berghöfer, T. W., & Christian, D. J., 2002, *A&A*, 384, 890
- Bonatto, C. & Bica, E., 2009, *MNRAS*, 394, 2127
- Castelli, F., & Hubrig, S., 2004, *A&A*, 425, 263
- Chen, L., de Grijs, R., & Zhao, J. L., 2007, *AJ*, 134, 1368
- Crawford, D. L., 1978, *AJ*, 83, 48
- J. Daszyńska-Daszkiewicz, J., Dziembowski, W. A., Pamyatnykh, A. A., & Goupil, M. -J., 2002, *A&A*, 392, 151
- De Cat, P., 2007, *CoAst*, 150, 167
- Dziembowski, W. A., Moskalik, P. & Pamyatnykh, A. A., 1993, *MNRAS*, 265, 588
- Flower, P. J., 1977, *A&A*, 54, 31
- Flower, P. J., 1996, *ApJ*, 469, 355
- Gautschi, A., 2009, *A&A*, 498, 273
- Gautschi, A. & Saio, H., 1993, *MNRAS*, 262, 213
- Gruber, D., Lachowicz, P., Bissaldi, E., Briggs, M. S., Connaughton, V., Greiner, J., van der Horst, A. J., Kanbach, G., Rau, A., Bhat, P. N., Diehl, R., von Kienlin, A., Kippen, R. M., Meehan, C. A., Paciesas, W. S., Preece, R. D. & Wilson-Hodge, C., 2011, *A&A*, 533, 61
- Handler, G., 2011, *A&A*, 528, 148
- Heiser, A.M., 1977, *AJ*, 82, 973
- Hensberge, H., Pavlovski, K. & Verschueren, W., 2000, *A&A*, 358, 553
- Huang, W. & Gies, D. R., 2006, *ApJ*, 648, 591
- Kallinger, T., Reegen, P. & Weiss, W. W., 2008, *A&A*, 481, 571
- Kaltcheva, N. T., Olsen, E. H., & Clausen, J. V., *A&A*, 353, 605
- Kaufer, A., Stahl, O., Tubbesing, S., et al., 2000, *SPIE*, 4008, 459
- Kharchenko, N. V., Piskunov, A. E., Röser, S., Schilbach, E., & Scholz, R.-D. 2004, *AN*, 325, 740
- Kharchenko, N. V., Piskunov, A. E., Röser, S., Schilbach, E., & Scholz, R.-D. 2005, *A&A*, 438, 1163
- Kołaczkowski, Z., Pigulski, A., Soszyński, I., Udalski, A., Kuźbiak, M., Szymański, M.; Żebruń, K., Pietrzyński, G., Woźniak, P. R., Szewczyk, O., & Wyrzykowski, Ł., 2006, *Memorie della Societa Astronomica Italiana*, 77, 336
- Lenz, P. & Breger, M. *CoAst.*, 146, 53
- Lee, U. & Baraffe, I., *A&A*, 301, 419
- Marschall L.A., van Altena W.F., & Chiu L.T.G., 1982, *AJ*, 87, 1497
- Mermilliod, J.-C. & Paunzen, E., 2003, *A&A*, 410, 511
- Moon, T., Dworetzky, M.M., 1985, *MNRAS*, 217, 305
- Napiwotzki, R., Schönberner, D. & Wenske, V., 1993, *A&A*, 268, 653
- Niemczura, E., private communication
- Ogura, K. & Ishida, K., 1981, *PASJ*, 33, 149
- Palla, F. & Stahler, S. W., 1993, *ApJ*, 418, 414
- Palla, F. & Stahler, S. W., 2000, *ApJ*, 540, 255
- Park, B.-G., & Sung, H. 2002, *AJ*, 123, 892
- Perez, M.R., The, P.S., & Westerlund, B.E., 1987, *PASP*, 99, 1050
- Perez, M.R., Joner, M. D., The, P.S., & Westerlund, B.E., 1989, *PASP*, 101, 195
- Reegen, P., Kallinger, T., Frast, D., Gruberbauer, M., Huber, D., Matthews, J.M., Punz, D., Schraml, S., Weiss, W.W., Kuschnig, R., Moffat, A.F.J., Walker, G.A.H., Guenther, D.B., Rucinski, S.M. & Sasselov, D. 2006, *MNRAS*, 367, 1417
- Saio, H., Kuschnig, R., Gautschi, A., Cameron, C., Walker, G. A. H., Matthews, J. M., Guenther, D. B., Moffat, A. F. J., Rucinski, S. M., Sasselov, D., & Weiss, W. W. 2006, *ApJ*, 650, 1111
- Sbordone, L., 2005, *MSAIS*, 8, 61
- Vaughan, S., 2005, *A&A*, 431, 391
- Waelkens, C., 1987, *Meded. K. Acad. Wet., Lett. Schone Kunsten Belg.*, 49, 59
- Waelkens, C., 1991, *A&A*, 246, 453
- Waelkens, C., & Rufener, F., 1985, *A&A*, 152, 6
- Walker, G. A. H., Matthews, J.M., Kuschnig, R., Johnson, R., Rucinski, S., Pazder, J., Burley, G., Walker, A., Skaret, K., Zee, R., Grocott, S., Carroll, K., Sinclair, P., Sturgeon, D., & Harron, J. 2003, *PASP*, 115, 1023
- Walker, G. A. H., Kuschnig, R., Matthews, Cameron, C., Saio, H., Lee, U., Kambe, E., Masuda, S., Guenther, D. B., Moffat, A. F. J., Rucinski, S. M., Sasselov, D., & Weiss, W. W., 2005, *ApJ*, 635, 77

APPENDIX A: INSTABILITY RANGE FOR G-MODES IN PMS STARS

Since PMS evolutionary tracks of intermediate masses ($3 \lesssim M/M_{\odot} \lesssim 6$) enter into a g-mode instability region (i.e., the SPB instability region) caused by the Fe opacity bump at $T \approx 1.5 \times 10^5$ K, certain g-modes can theoretically be excited in some intermediate PMS stars. We have examined the instabilities of nonradial g-mode oscillations of $\ell = 1$ and 2 for PMS models

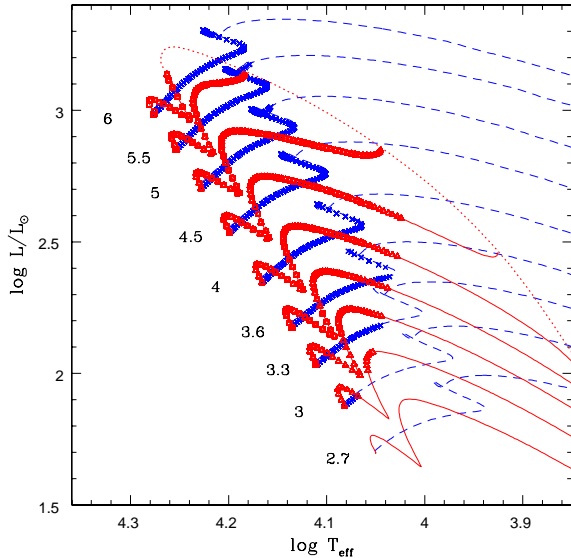


Figure A1. Models in which g-modes are excited are indicated by symbols (\triangle and \square for $\ell = 1$ and 2 modes, respectively for PMS models, and \times for both ℓ s for main-sequence models) along evolutionary tracks with various masses. Red solid lines indicate PMS models, while blue dashed lines main-sequence and post-main sequence models. Dotted line indicates evolutionary tracks during mass-accreting proto-stellar evolution.

with masses ranging across $2.7 M_{\odot}$ to $6 M_{\odot}$. The initial models for the evolution of each mass were obtained by accreting mass at a rate of $10^{-5} M_{\odot} \text{yr}^{-1}$ starting from a fully convective $1 M_{\odot}$ model. Those initial models are roughly located on the birth-line of PMS stars (Palla & Stahler 1993).

The stability results are shown in Fig. A1, where red triangles and squares indicate the positions of models in which g-modes are excited. Red lines indicate the evolutionary tracks of PMS stars, while blue lines are main-sequence and post-main-sequence tracks. Main-sequence models unstable to g-modes (corresponding to what would be currently recognised SPB stars) are highlighted by blue crosses.

Because the Brunt-Väisälä frequency becomes very high in the core of a post-main-sequence star, g-modes are damped due to dissipation unless a shell convection zone appears, as in massive stars (Saio et al. 2006; Gautschy 2009). This is why the instability range for prototype SPB stars is confined to the MS band (Gautschy & Saio 1993; Dziembowski et al. 1993). In PMS stars, however, g-modes survive even in the phase without core convection, because the Brunt-Väisälä frequency in the interior is not as high as in a post-main-sequence star. The spatial wavelength of the eigenfunction is therefore too long for the dissipation to be important. (The number of nodes of excited g-modes is well below 100.) As a result, the g-mode instability range for PMS stars (red symbols in Fig. A1) is broader than that for MS SPB stars (blue symbols). The models predict PMS SPB stars which overlap with and extend beyond the main sequence band in the HR Diagram.